

# ME338 – MANUFACTURING PROCESSES II

Project Report

## Modelling of Laser Cladding Process

DARSHIL DESAI	160020018
MANOJ PARMAR	150100021
MRUNMAYI MUNGEKAR	160020012
TANYA GUPTA	150040010

Under the Guidance of:

Prof R.K. Singh



Department of Mechanical Engineering  
INDIAN INSTITUTE OF TECHNOLOGY, BOMBAY

2018

# INDEX

---

1. Abstract
2. Problem Discussion
3. Literature Review
4. Temperature Modelling
5. Heat Affected Zone
6. Results and Discussion
7. Future Scope
8. References

# ABSTRACT

---

Laser Cladding or Laser Deposition is a processing technique used for adding one material to the surface of another in a controlled manner. A stream of a desired powder is fed into a focused laser beam as it is scanned across the target surface, leaving behind a deposited coating of the chosen material. This enables the applied material to be deposited selectively just where it is required.

Preliminary Objectives:

1. Analyze a model to predict the temperature distribution of the Laser cladding process
2. Calculate dimensions of the Heat – Affected Zone and dilution
3. Code various phenomenological equations to estimate some or all the following secondary variables:
  - a. Hardness
  - b. Phase Transformations and its effects
  - c. Grain size

The time-dependent temperature fields developed during laser cladding are investigated in order to explain the cause of microcracking of the laser-cladded metallic coatings. The effect of base material preheating on the cracking susceptibility is considered. An efficient approach is proposed, allowing one to calculate numerically the thermal and strain–stress distributions.

The temperature distribution would be computed using either ADINA or ANSYS. The other factors would be calculated after we get the basic temperature distribution.

We plan to conduct the Laser Cladding simplified process experimentally to compare values of some specifically chosen points with the calculated Temperature/Stress values.

# PROBLEM DISCUSSION

---

There are various advantages of a laser cladding process, a few of them being additional material can be placed precisely where desired, a very wide choice of different materials can be deposited, deposits are fully fused to the substrate with little or no porosity and minimal heat input results in narrow HAZ (heat affected zone). The process produces a strong metallurgical bond with minimal dilution of the base material for enhanced corrosion, abrasion and wear resistance of metals.

As the change of temperature is very steep and the molten pool formed is very small, it is difficult to measure the temperature distribution in the molten pool through experiment. Therefore, the method of numerical simulation is widely adopted. This is what we will be focusing on in our project. Due to the uneven temperature field, the local plastic deformation in the cladding process, and the differences of thermal expansion property between the substrate and the cladding material, huge residual stress can result in the remanufactured parts. Different laser cladding parameters can lead to different temperature field. The temperature distribution characteristics of laser cladding remanufacturing are important for optimizing the parameters of laser cladding and improving the quality of cladding layer.

When selecting powder, several factors such as the following should be considered:

1. The cladding powder should have a good formability and a good wettability with the substrate.
2. The mechanical properties and physical properties of powder are similar to the substrate, which can satisfy the work condition of the impeller.
3. The chemical composition and thermal physical properties of powder are similar to that of the substrate

After extensive analysis literature review and discussion, we came to the conclusion that with the constrains we were operating in we could work with the temperature simulation and the calculation of the heat affected zone. The secondary variables like grain size, hardness and phase transformation analysis could be taken up ahead in the future.

# LITERATURE REVIEW

---

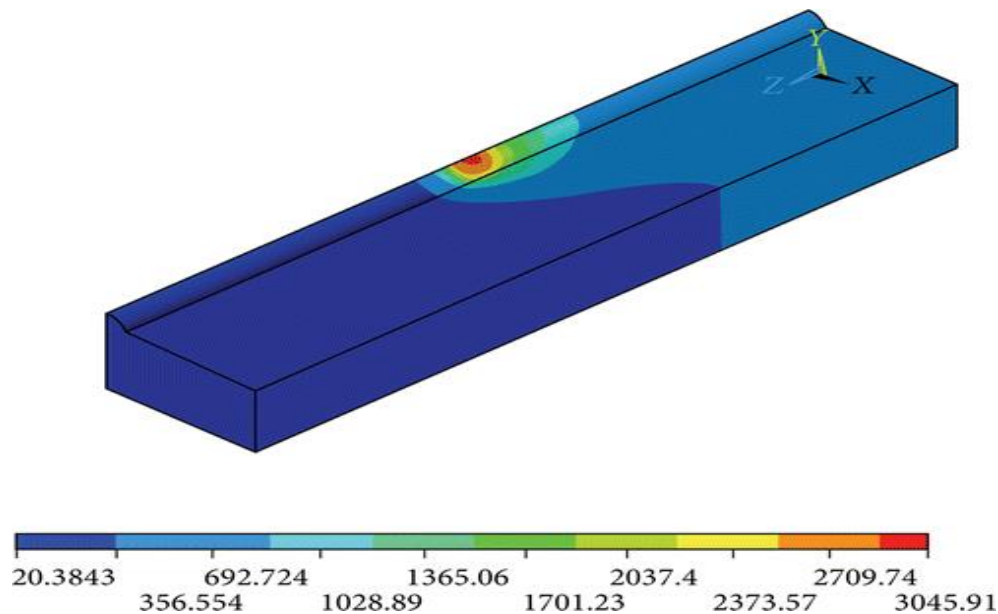


**Fig 1:** Temperature simulation for one half of cladding due to symmetry

Our literature review of the topic spanned across various papers describing the modelling of temperature and residual stress distribution in the process of laser cladding. Research on this topic dates way back in the history of manufacturing.

In the 90s, A. F. A. Hoadley and M. Rappaz worked on a thermal model for laser manufacturing via power injection. This paper described a two-dimensional model for laser cladding in contrast to today's 3D demands. The thermal distribution of the cross-sectional part of the laser clad has been studied. The effect due to the injected powder is considered. This is done by considering the immediate melting of the powder into the liquid metal. Consequently, the heat required for the phase transformation of the powder is uniformly distributed throughout the melt and is a part of the convection process of the thermal study. On modelling the temperature distribution, they studied various factors associated with this such as the occurring dilution. Dilution occurs when the temperature at the point goes beyond the melting point of the base metal. They came upon an optimal value for the cladding speed by taking into account the dilution such that for lower speed the depression of the base material, i.e. the dilution is high whereas on faster cladding you would find that the clad sticking isn't very strong. The main takeaway from this process was that the powder mass and energy transfer properties weren't needed to be studied separately as the powder mixing was considered instantaneous.

In 2011, Fang LUO, Jian-hua YAO, Xia-xia HU and Guo-zhong CHAI demonstrated the effect of the laser power on the cladding temperature and the heat affected zone or the HAZ. They used a CO2 laser power for cladding a P20 steel base metal. The powder used for the process was tool steel powder H13. They observed that for lower laser powers the heat absorption and consequent temperature increase of the laser clad is low. This leads to incomplete melting of the coating powder. This then results in a lesser size of the heat affected zone around the cladding. On the contrary for high powers, the liquefied metal region increases in size thus, ensuring complete melting of the powder and hence, a larger heat affected zone. Thus, this paper described the variation in the cladding temperature as the laser power is changed, and its effect on the metal liquid pool and consequently on the surrounding, non-melted, heat affected zone.

Later in 2015, Liang Hua, Wei Tian, and Wenhe Liao, performed a similar study on of the thermal and residual stress distribution during laser cladding. They performed a 3D finite element method by using a 48 mm × 20 mm × 5 mm base of 16MnR with a powder coating of Ni-Cr-B-Si. With a clad of radius 1mm, they exploited the symmetry of the sample by using only half the sample for modelling. Their thermal modelling was based on the following partial differential equation in terms of

$$\rho c \frac{\partial T}{\partial t} = \frac{\partial}{\partial x} \left( \lambda \frac{\partial T}{\partial x} \right) + \frac{\partial}{\partial y} \left( \lambda \frac{\partial T}{\partial y} \right) + \frac{\partial}{\partial z} \left( \lambda \frac{\partial T}{\partial z} \right) + Q,$$

**Fig 2:** Partial derivative equation considering heat source Q and temperature variation

the density, thermal capacity, thermal conductivity, the latent heat of phase transformations and the position-time dependence. With very high temperatures, they have taken into account both radiative as well as convective heat transfer along with conduction. They modified the normal equation of a Gaussian heat source to a double ellipsoid one, to account for the heat deposited in the front and the rear of the cladding bead. This was necessitated by the inability of the Gaussian two-dimensional source to provide an understanding of the depth at which the laser heat goes during the cladding. They observed elliptical isotherms (half-elliptical as they worked with only half the sample) with higher temperature gradients in front of the laser beam. Like previous papers, they concluded a deeper HAZ, with high laser power and slower speeds. Moreover, they established a variation of the same with the laser spot diameter concluding that a smaller diameter consistently implies a larger HAZ.

Going through these and many other papers, we decided to try out modelling the laser cladding process ourselves to get an idea of how temperature varies across the sample.

# TEMPERATURE SIMULATION MODELLING

The modelling of the laser cladding process was done in ANSYS. The tool powder was chosen to be H13 high speed steel and the size of the substrate was 5x5x7mm. The modelling was done using element birth technique wherein a semi-circular clad was chosen with a diameter of 1.2mm. Now, the substrate was divided into 4 equal parts to simulate the moving laser cladding process. A laser with a given power (100W) was focussed on the centre of those 4 parts for a time interval of 1 second each, i.e., the velocity of the laser was assumed to be known. Hence, the total simulation time was 4 seconds (1 second for each part). Hence, a good approximation of the transient thermal states can be obtained by assuming the clad to be divided into many parts and then moving the laser on each one of them subsequently. The simulation was done for different powers of laser and the corresponding maximum and minimum temperature were obtained.

Major Assumptions in the model are:

- Material is isotropic in nature.
- The flow function of molten pool fluid is neglected.
- Heat loss due to radiation is not accounted for in the model.
- Evaporation of the substrate and the powder is neglected.

Properties used:

Thermal conductivity (K) = 26.4W/mK

Specific heat capacity ( $C_p$ ) = 490 W/kgK

Density ( $\rho$ ) = 7448 kg/m<sup>3</sup>

Melting Temperature ( $T_m$ ) = 1700 K

Convection coefficient (h) = 15 W/m<sup>2</sup>K

Latent heat of fusion (L) = 320 KJ

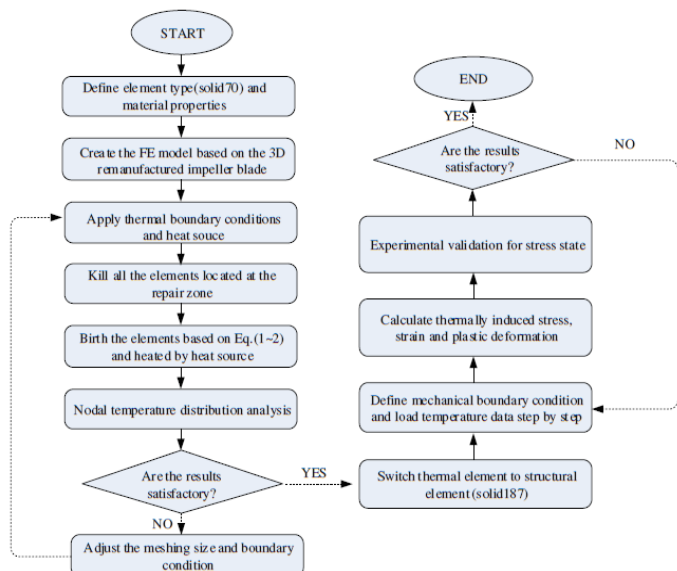


**Fig 3:** Bringing structure in our analysis

# HEAT AFFECTED ZONE

Approximation: The fused or the Heat Affected Zone (HAZ) is assumed to be circular in nature. Width and height of both the clad bead and fused zone has been measured using co-ordinate option provided in Ansys fluent result section. Readings are noted down in Microsoft Excel.

## Sample Calculation:

Power supplied: 1000 W

Height of clad bead: 1.2 mm

Width of clad bead: 1.2 mm

Height of HAZ formed: 1.893 mm

Width of HAZ formed: 2.578 mm

## For HAZ

Radius of HAZ formed, R2: 1.289 mm

Area of HAZ, A2: 3.08039 mm<sup>2</sup>

## For clad bead

Radius of clad bead, R1: 0.75 mm

Area of clad bead, A1: 1.51554 mm<sup>2</sup>

## Dilution, D

$$D(\%) = \frac{A2}{A2 + A1} * 100 = 67.024\%$$

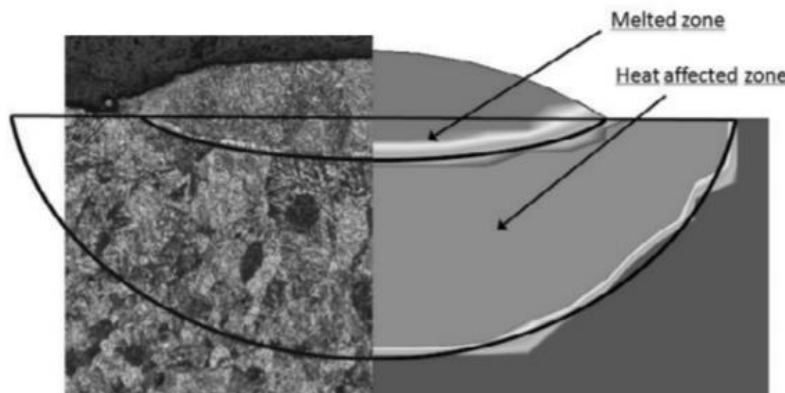


**Fig 4:** A modelled heat affected zone (HAZ)

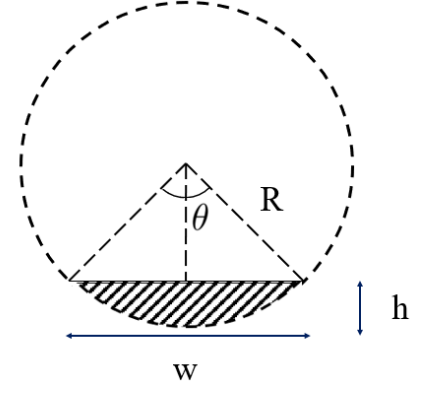


## Formula derivation:

Area calculation for given height  $h$  and width  $w$

Calculation for  $R$ :

$$\begin{aligned} R^2 &= (R - h)^2 + \frac{w^2}{4} \\ \Rightarrow R^2 &= R^2 + h^2 - 2Rh + \frac{w^2}{4} \\ \Rightarrow R^2 &= \frac{h^2 + \frac{w^2}{4}}{2h} = \frac{w^2 + 4h^2}{8h} \end{aligned}$$



When  $h < R$ , Area ( $A$ ) =

$$\begin{aligned} & \left(\frac{\theta}{2\pi}\right)\left(\frac{\pi R^2}{4}\right) - \frac{1}{2}w(h - R) \\ & \sin \frac{\theta}{2} = \frac{(\frac{w}{2})}{R} \\ & \theta = 2\sin^{-1} \frac{w}{D} \end{aligned}$$

When  $h > R$ ,  $A =$

$$\begin{aligned} & \pi R^2 - \left(\left(\frac{\theta}{2\pi}\right)\left(\frac{\pi R^2}{4}\right) - \frac{1}{2}w(h - R)\right) \\ & \text{where, } \theta = 2\sin^{-1} \frac{w}{D} \end{aligned}$$

## Sample Calculations

Fused zone: Width ( $w$ ) = 2.578mm

Depth ( $h$ ) = 1.893mm

For calculating area, we need to first find the radius of the circle for which this depth and height are part of:

$$\text{So, } R^2 = \frac{w^2 + 4h^2}{8h} = \frac{(2.578)^2 + 4(1.893)^2}{8(1.893)} = 1.289\text{mm}$$

Since  $h > R$ , Area

$$\begin{aligned} & \pi R^2 - \left(\left(\frac{\theta}{2\pi}\right)\left(\frac{\pi R^2}{4}\right) - \frac{1}{2}w(h - R)\right) \\ & \theta = 2\sin^{-1} \frac{w}{D} = 1.1956 \\ & A_2 = \pi(1.289)^2 - \left(\left(\frac{1.1956}{2\pi}\right)\left(\frac{\pi(1.289)^2}{4}\right) - \frac{1}{2}(2.578)(1.893 - 1.289)\right) \\ & A_2 = 3.08039\text{mm}^2 \end{aligned}$$

For melt pod, Width ( $w$ ) = 1.2mm

Depth ( $h$ ) = 1.2mm

$$\text{So, } R^2 = \frac{w^2 + 4h^2}{8h} = \frac{(1.2)^2 + 4(1.2)^2}{8(1.2)} = 0.75\text{mm}$$

Since  $h > R$ , Area =

$$\begin{aligned} & \pi R^2 - \left(\left(\frac{\theta}{2\pi}\right)\left(\frac{\pi R^2}{4}\right) - \frac{1}{2}w(h - R)\right) \\ & A_1 = 1.51554\text{mm}^2 \end{aligned}$$

Dilution % =

$$\begin{aligned} & \frac{A_2}{A_1 + A_2} = \frac{3.08039}{1.51554 + 3.08039} * 100 \\ \Rightarrow & \text{Dilution}\% = 67.024 \end{aligned}$$

Data points has been collected from simulation for four different clad bead heights,  $h$  and different laser power inputs,  $P$  which has been listed

i) Clad bead of height,  $h = 0.8$  mm and width 1.2 mm

power(W)	width of HAZ $w$ (mm)	depth of HAZ $h$ (mm)	Radius of clad deposited(mm)
1000	1.3368	0.4506	0.625
600	1.208	0.0727	0.625

ii) Clad bead of height,  $h = 1$  mm and width 1.2 mm

power(W)	width of HAZ $w$ (mm)	depth of HAZ $h$ (mm)	Radius of clad deposited(mm)
1000	1.8655	1.00379	0.68
600	1.48126	0.56594	0.68
400	1.25206	0.24927	0.68
350	1.22638	0.14664	0.68

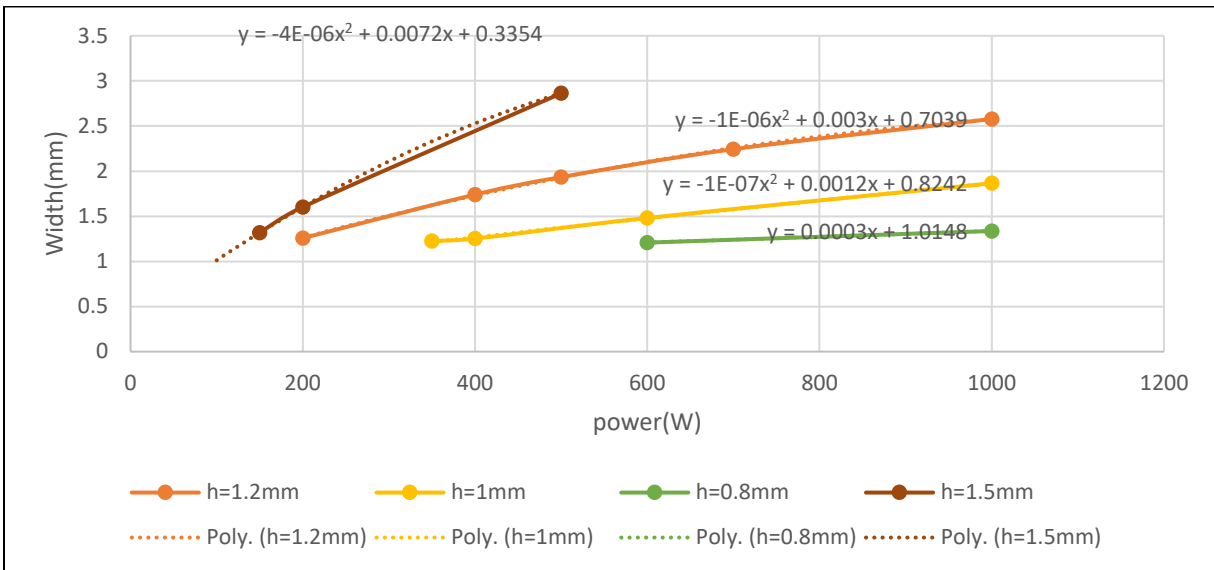
iii) Clad bead of height,  $h = 1.2$  mm and width 1.2 mm

power(W)	width of HAZ $w$ (mm)	depth of HAZ $h$ (mm)	Radius of clad deposited(mm)
1000	2.578	1.893	0.75
700	2.2436	1.4943	0.75
500	1.9338	1.1021	0.75
400	1.7402	0.93503	0.75
200	1.25768	0.2893	0.75

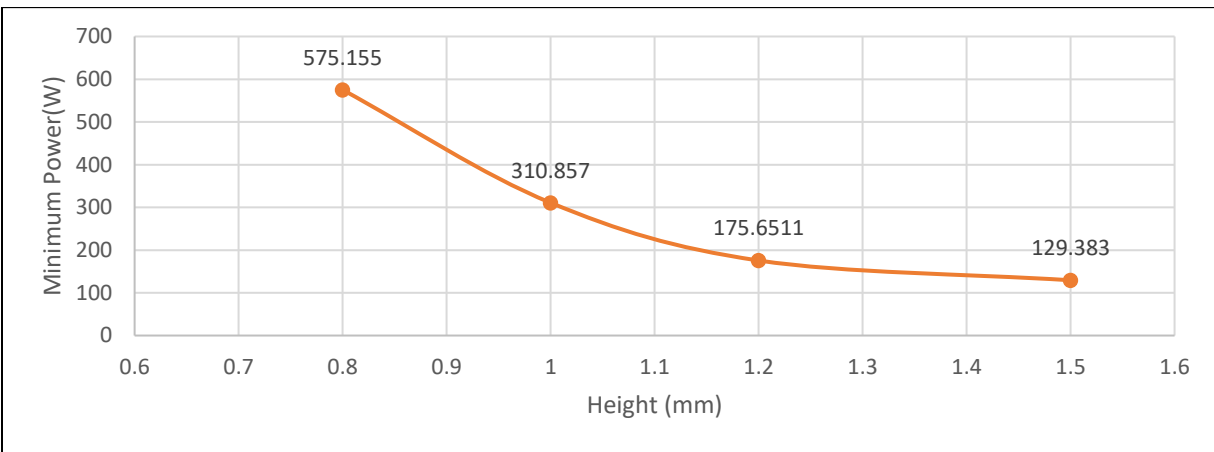
iv) Clad bead of height,  $h = 1.5$  mm and width 1.2 mm

power(W)	width of HAZ $w$ (mm)	depth of HAZ $h$ (mm)	Radius of clad deposited(mm)
500	2.86198	1.62152	0.87
200	1.60274	0.63671	0.87
150	1.318	0.3274	0.87

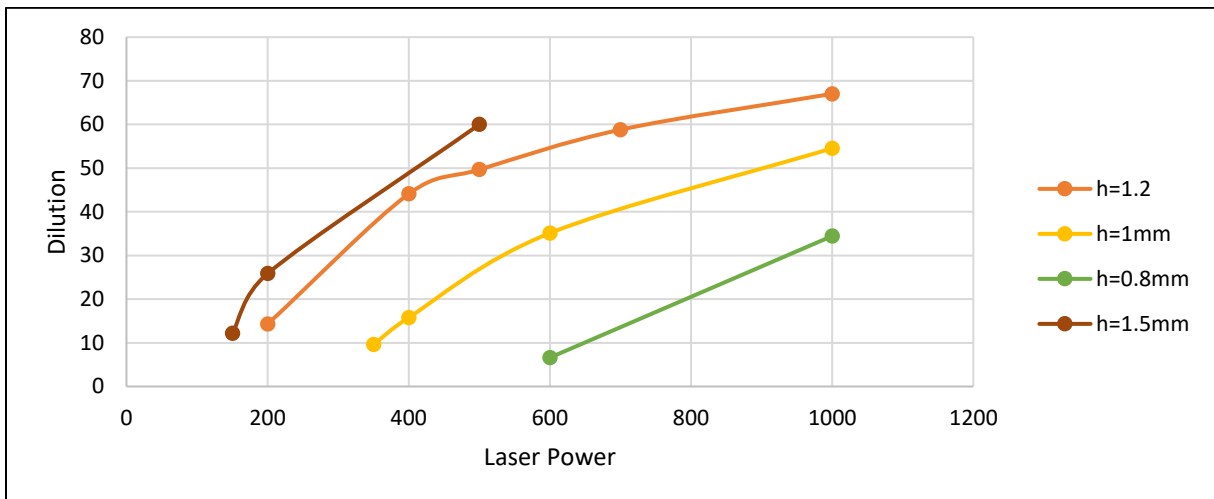
## Modelling for Laser Cladding Process



Graph: Width of HAZ vs Laser Power



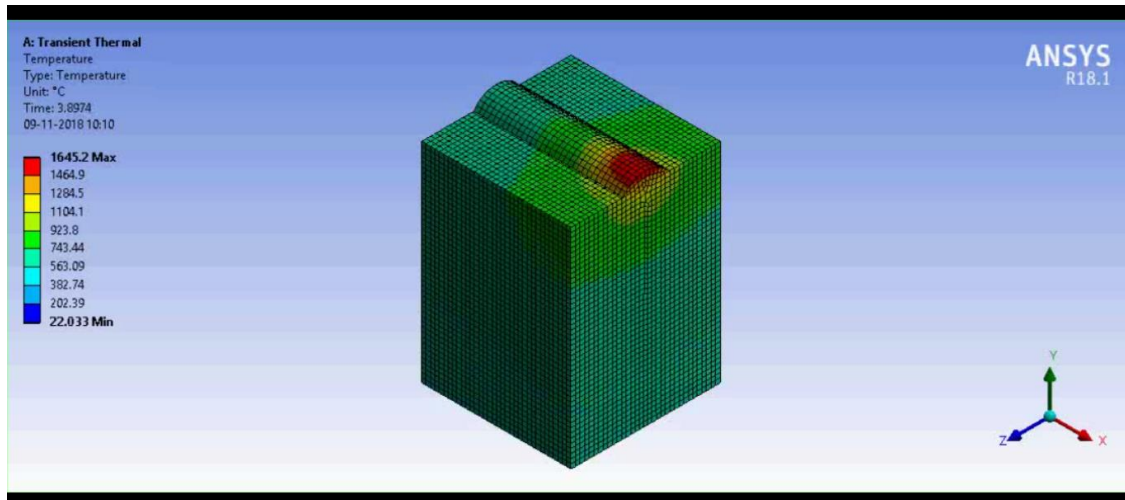
Graph: Minimum power vs Height of HAZ



Graph: Dilution percentage vs Laser power

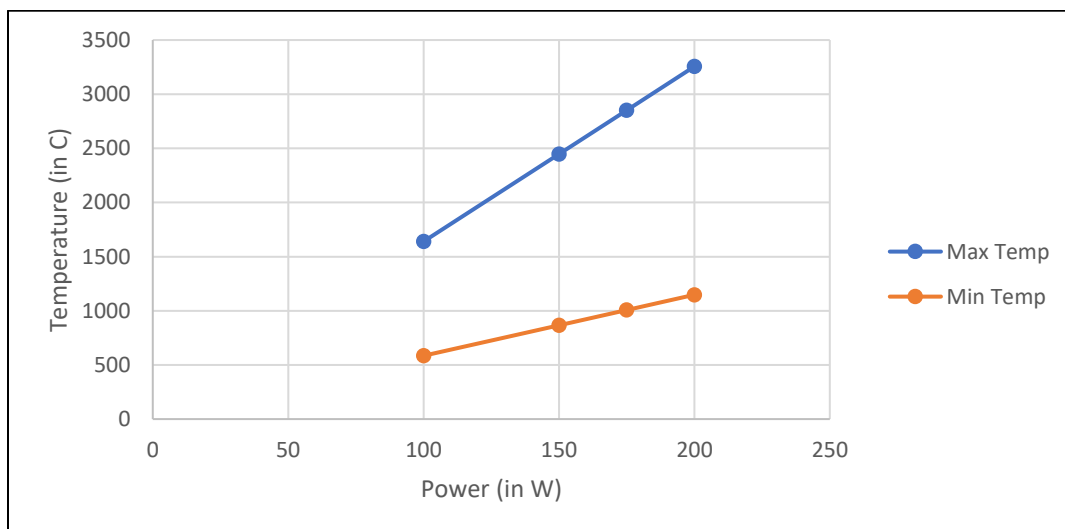
# RESULTS AND DISCUSSION

The figure given below is a screenshot of simulation of the laser cladding process with input power of 100W



The maximum and minimum temperatures obtained for different power inputs:

Power (W)	Max Temperature (°C)	Min Temperature (°C)
100	1640	585
150	2447	866
175	2851	1007
200	3256	1148



In Graph: Temperature vs Laser Power

For the temperature simulation, we observe that the maximum and minimum temperature increase with the laser power, which seems obvious as a laser of higher power would release more heat.

For the HAZ modelling, observations for different heights of the heat affected zone are made, dilution and width increase with laser power for all heights. Also, the minimum power decreases almost exponentially with the height of HAZ and becomes constant after 1.5mm.

Since we have not conducted the experiment, we have not verified the observations ourselves. But our observations and hence conclusions are in line with existing literature.

# FUTURE SCOPE

---

Future investigations could revolve around analysis of how different parameters including but not limited to beam diameter, processing speed, speed of the particles and powder feed rate affect the temperature distribution. We were limited in our analysis since we checked for variation with laser power only.



**Fig 5:** Sample cladding process

ANSYS is a powerful modelling environment to work in, and we were unable to fully utilize the resources it provides. The effect of convection has been considered, while we have ignored radiation, due to the high temperatures it will also contribute to temperature distribution variation and its effect on the heat transfer in the melt pool could be considered for future work. The powder feeding system can also be modelled allowing prediction of clad height and powder temperature distribution in a single model.

Our original scope for work involved analysis of secondary variables which we would like to continue building upon. For phase transformation variation during the laser cladding process, we went through several papers. One of them was by Yiwen Lei, Ronglu Sun and Wei NiuAn. They used an X-ray diffractometer and scanning electron microscope with energy dispersive spectroscopy to analyze the microstructure and phase compositions of the coating. Thermodynamic calculation was performed with Thermo-Calc software based on a commercially available Alloys' database. The experimental results show that. The calculated results and experimental data indicated how the solidification process in the coating during laser cladding process proceeded from one phase to another. A solid-state phase transformation occurred after the solidification process.

It's difficult to capture the temperature variation as discussed before, but we have seen great strides being made in technology and one of the potential methods include use of image processing during the process. This camera could be previously calibrated with a black body and it enables the surface temperature to be obtained. We can also obtain geometrical features of the track such as height and width in real time and obtain information related to the process parameters, and hence calculate the HAZ. Using this would also help us verify our simulations experimentally.

# REFERENCES

---

1. <http://www.lasercladding.co.uk/Laser-Cladding-Process.aspx>
2. <https://www.sciencedirect.com/science/article/pii/S0045794904000033>
3. <https://journals.sagepub.com/doi/full/10.1155/2014/291615>
4. <https://link.springer.com/content/pdf/10.1007%2Fs00170-016-9445-z.pdf>
5. <https://www.sciencedirect.com/science/article/pii/S1006706X11600149>
6. <https://www.sciencedirect.com/science/article/pii/S0143816603000630>
7. <https://link.springer.com/article/10.1007/BF02649723>
8. <https://www.ipgphotonics.com/en/applications/materials-processing/cladding>
9. [http://www.le2i.cnrs.fr/IMG/publications/130\\_Lasers%20in%20engineering-97.pdf](http://www.le2i.cnrs.fr/IMG/publications/130_Lasers%20in%20engineering-97.pdf)
10. [https://ac.els-cdn.com/S1875389211001623/1-s2.0-S1875389211001623-main.pdf?\\_tid=3ae4cdd4-bd64-46cf-aeb2-56c81cf1822c&acdnat=1542698366\\_9f6851afde5016d23dd8e935d93271c2](https://ac.els-cdn.com/S1875389211001623/1-s2.0-S1875389211001623-main.pdf?_tid=3ae4cdd4-bd64-46cf-aeb2-56c81cf1822c&acdnat=1542698366_9f6851afde5016d23dd8e935d93271c2)